Glycoconj J (2009) 26:1109–1116
DOI 10.1007/s10719-009-9231-3

Novel mannosidase inhibitors probe glycoprotein degradation pathways in cells

Terry D. Butters · Dominic S. Alonzi · Nikolay V. Kukushkin · Yuan Ren · Yves Blériot

Received: 9 December 2008 / Revised: 14 January 2009 / Accepted: 27 January 2009 / Published online: 21 February 2009

Abstract Multiple isoforms of mammalian α-mannosidases are active in the pathways of N-linked glycoprotein synthesis and catabolism. They differ in specificity, function and location within the cell and can be selectively inhibited by imino sugar monosaccharide mimics. Previously, a series of structurally related novel 7-membered iminocyclitols were synthesised and found to be inhibitors of α-mannosidase using *in vitro* assays. The present study aimed to delineate α-mannosidases hydrolytic pathways in azepane inhibitor treated cells by the analysis of free oligosaccharides (FOS) as markers of endoplasmic reticulum (ER), Golgi, lysosomal and cytosolic α-mannosidase activities. Two compounds were identified as potent and selective cytosolic α-mannosidase inhibitors. Two related compounds were shown to be potent inhibitors of lysosomal α-mannosidase with different potencies towards α1,6 mannosidase. The specificities of these novel 7-membered imino sugars are related to differences in their structure and D-mannose-like stereochemistry. Specific ER-mannosidase inhibition by kifunensine also reveals significant non-proteasomal degradation following FOS analysis and appears to be cell line dependent. The availability of more selective inhibitors allows the pathways of N-linked oligosaccharide metabolism to be dissected.

T. D. Butters (✉) · D. S. Alonzi · N. V. Kukushkin · Y. Ren
Oxford Glycobiology Institute, Department of Biochemistry,
University of Oxford,
South Parks Road,
Oxford OX1 3QU, UK
e-mail: terry.butters@bioch.ox.ac.uk

Y. Blériot
Glycochemistry group,
Institut Parisien de Chimie Moléculaire (IPCM) UMR-CNRS 7201,
Université Pierre et Marie Curie—Paris 06,
4 place Jussieu,
7500 Paris, France

Keywords Lysosomal · Cytosolic · Oligosaccharides · Endoplasmic reticulum associated degradation

Introduction

Mammalian α-mannosidases play important roles in glycoprotein biosynthesis, quality control and catabolism [1]. There are multiple forms of mammalian α-mannosidases that differ in their specificity, function and location within the cell. They are thought to have evolved from two primordial genes in order to generate a more efficient system of protein folding and to compliment the increasingly complex role of glycans in cellular processes [1].

A range of furanose and pyranose imino sugar analogues have been found to inhibit these α-mannosidases with target specificities based on subtle differences in their structure and stereochemistry [2]. Hence, they can selectively block steps in mannosidase pathways and alter glycan structures intra- and extracellularly. Imino sugars have been used to progress our understanding of these pathways and have great potential as therapeutic drugs [3]. Swainsonine is a potent inhibitor of Golgi α-mannosidase II, reduces tumour cell metastasis and solid tumour growth in mice and has been evaluated in a Phase 1B trial for patients with advanced malignancies [4].

A new series of compounds based upon an N-alkylated polyhydroxylated azepane scaffold have been synthesised with D-glucose and L-idose-like configuration [5]. These were found to be potent ß-glucosidase inhibitors with weak activity towards α-glucosidases and α-mannosidases using *in vitro* assays [5].

A series of α1, 2-mannosidases involved in the trimming or 'processing' of high mannose oligosaccharides are essential for maturation as they produce the substrate

required for the formation of hybrid and complex glycans [6]. ER α-mannosidase I and II initiate trimming of the polymannose structure by cleaving a single α1,2-mannose and in the Golgi, at least two α-mannosidase I isoforms can trim a $Man_{8-9}GlcNAc_2$ ($M_{8-9}N_2$) *N*-linked glycan to $Man_5GlcNAc_2$ (M_5N_2).

ER associated degradation (ERAD) is a normal cellular 'quality control' mechanism to ensure early retention and destruction of misfolded proteins in order to prevent their maturation [7]. Misfolded proteins are retained in the ER and retro-translocated into the cytosol possibly through the Sec61 channel [8]. ER α-mannosidase I can act as a 'timer' for persistently misfolded proteins, due to its slow *in vivo* activity [7] and its product acts as a ligand for a specific receptor EDEM, which selectively binds misfolded glycoproteins and targets them for ERAD [7, 9]. The glycan moiety is released by a peptide:*N*-glycanase (PNGase) in the cytosol to produce a free oligosaccharide (FOS) with a *N*-acetylchitobiose at the reducing end ($GlcNAc_2$; N_2). An endo-β-α-*N*-acetylglucosamine (ENGase) cleaves between the $GlcNAc_2$ (N_2) to produce a single GlcNAc (N_1) [10]. The resulting FOS acts as a substrate for cytosolic α-mannosidase which is derived from the same gene MAN2C1 as ER mannosidase II [11].

There is also evidence for an alternative non-proteasomal ERAD pathway in the lumen of the ER where a luminal isoform of PNGase releases the oligosaccharide from the protein [7].

In addition to catabolic products found in the cytosol, all glycoproteins containing high-mannose, hybrid and complex glycans are catabolised in the lysosome [12]. A combination of lysosomal proteases and glycosidases act bidirectionally in a highly ordered process. Lysosomal α-mannosidase is ubiquitously found in eukaryotic cells, and a deficiency causes the accumulation of mannose-rich storage products that can result in the lysosomal storage disease α-mannosidosis. In humans, there is an additional residual lysosomal α1,6 mannosidase activity, which has high specificity for the core tetrasaccharide $Man_3GlcNAc_1$ (M_3N_1) [13]. Lysosomal mannosidase and α1,6-mannosidase work in conjunction to achieve the efficient catabolism of *N*-glycans.

A lysosomally located *N*-acetylchitobiase (ENGase) is expressed in humans and rodents but not in ungulates, cats and dogs [12]. This is indirectly demonstrated by the storage of $Man_nGlcNAc_2$ (M_nN_2) structures in bovine and feline mannosidosis compared to $Man_nGlcNAc$ (M_nN_1) structures in the human form [14].

Following preliminary experiments performed on the activity of novel azepane-based inhibitors in cells [5], it was evident that the detection of free oligosaccharides suggested that a number of mannosylated species were generated. These species have been characterised further and support the potential of analysing free oligosaccharides produced as a consequence of inhibition, to delineate pathways of glycoprotein biosynthesis and catabolism.

Methods

Materials

Reagents were from Sigma (Gillingham, UK) unless otherwise stated. Tissue culture media supplied by Gibco/Invitrogen (Paisley, UK). Water was Milli-Q™ grade. Non-alkylated parent compounds of inhibitors **1-4**, were *N*-butylated and purified as described [5]. The structures are shown in Fig. 1.

Cell culture

HL60s and MDBK cells were cultured in RPMI 1640 medium with 2 mM L-glutamine, 1% of a stock solution of 100 U/ml penicillin, 100 μg/ml streptomycin and 10% fetal calf serum (FCS). Cells were incubated with and without inhibitors for 24 h before analysis.

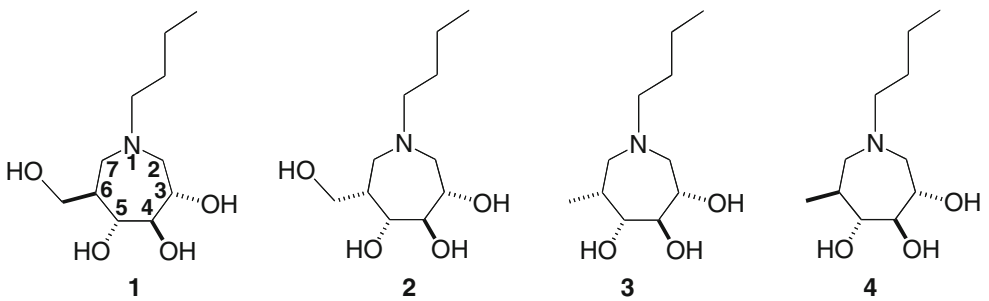

Fig. 1 Structures of *N*-butyl-azepane inhibitors **1-4.** The seven-membered imino sugars were synthesised following chemical transformation from a tri-*O*-benzylated six-membered azidolactol [5]. *N*-butylation of the tri- and tetra-hydroxylated azapanes generated derivatives (compounds **3**, **4** and **1**, **2** respectively) with modest inhibitory activity against glucosylceramide transferase and very weak activity against α-glucosidases [5]

Free oligosaccharide (FOS) extraction and labelling

Cells were grown to confluency, harvested and seeded at a lower density in fresh medium containing inhibitor at the required concentration and incubated for 24 h at 37°C.

Cells were washed with PBS by centrifugation, resuspended in 1 ml water and frozen at −20°C until required. Cell pellets were thawed and homogenised using a glass dounce homogeniser. An aliquot was taken for protein concentration determination and the remaining homogenate was desalted and deproteinated using mixed bed ion exchange chromatography [0.3 ml AG50W-X12 over 0.6 ml AG3-X4] as described [15]. FOS were 2-AA (anthranilic acid) labelled using methods previously developed [16].

Purification of fluorescently labelled FOS

The 2-AA labelled FOS was purified using a Concanavalin A (ConA)–Sepharose 4B column [15]. Small FOS were collected in the non-bound fraction and large (bound) FOS were eluted with hot 0.5 M α-methylmannoside [15].

Normal-phase high performance liquid chromatography (NP-HPLC) analysis of FOS

Purified 2-AA labelled FOS were separated by normal-phase high performance liquid chromatography using a previously published method [16]. Peak assignments were made based on glucose units determined from a glucose dextran ladder standard. Peak areas were calculated using Waters Empower software and converted into amounts using an experimentally derived factor and normalised to protein amount determined by BCA (bicinchoninic acid) assay using bovine serum albumin (BSA) as standard.

Isolation and analysis of glycoprotein derived N-linked oligosaccharides

HL60 cells were incubated with inhibitors at 100 μM for 24 h at 37°C. Cell pellets (1–2 mg protein) were harvested and washed with PBS and protein solubilised in 100 μl of 3% Triton X-114 (*v*/*v*) at 4°C. Samples were mixed and left on ice for 30 min and then mixed again and centrifuged at 12,000×*g* for 30 min at 4°C. Methanol (400 μl), was added to the supernatant followed by chloroform (100 μl) and water (300 μl), with mixing at each step. Following centrifugation at 12,000×*g* for 1 min the aqueous (top) and organic (lower) layers were removed leaving the protein precipitated at the interphase intact. This protein was denatured in 24 μl of 0.5% (*w*/*v*) SDS and 1% (*v*/*v*) 2-mercaptoethanol at 80°C for 30 min and after cooling, neutralised with 3 μl of 10% (*v*/*v*) NP-40 and 3 μl 0.5 M sodium phosphate buffer, pH 7.5. Aliquots (5 μl) were taken and 1 μl PNGase (500,000 U/ml, New England Biolabs, MA, USA), was added to digest the protein overnight at 37°C. Samples were made up to 30 μl with water and the released oligosaccharides labelled with 2AA and analysed by NP-HPLC as described above.

Flow Cytometry analysis of ConA binding to HL60 cells

Inhibitor treated HL60 cells were washed with PBS, resuspended in FACs (Florescence activated cell sorting) buffer (PBS containing 0.02 M sodium azide and 0.1% BSA) at 10^6 cells/well in a 96 well plate. A 20 μl aliquot (10 μg/ml) of ConA FITC (Vector Laboratories, Peterborough, UK) was added to each well and incubated on ice for 30 min. Cells were washed twice with 10% BSA in PBS, resuspended in FACs buffer containing 2 μg/ml propidium iodide (PI, Sigma-Aldrich) and the percentage of ConA labelled, PI non-labelled cells was determined by counting 10,000 events by flow cytometry (FACScalibur, Becton Dickinson, San Jose, CA, USA).

Results and discussion

Effect of α-mannosidase inhibitors on FOS in HL60 cells

MDBK cells are of bovine origin and have a lysosomal chitobiase deficiency [12]. As a consequence, lysosomally derived FOS are enriched in *N*-acetylchitobiose (N_2) core glycans. HL60 cells do not harbour this deficiency, so a comparison of FOS structures in these cell lines allows a superficial prediction of their location. Cytosolic FOS would predominantly contain a single *N*-acetylglucosamine reducing terminus (N_1) in both cell lines, whereas lysosomally-derived FOS would be mostly comprised of a chitobiose core reducing terminus (N_2) in MDBK cells. HL60 cell lysosomes could contain both N_1 and N_2 core oligosaccharides (see Table 1).

Compounds **1** and **2** had very similar patterns of FOS species indicating α-mannosidase inhibition in HL60 cells (Fig. 2B, C) although there were differences in relative potency. Following treatment for 24 h with 100 μM **1** and **2**, the total FOS levels increased from 347±61 (pmol/mg) in control cells to 868±177 and 678±76 (pmol/mg) in inhibitor treated cells, respectively. In particular, the $M_{6-9}N_{1-2}$ species (Peaks 10 to 17, Fig. 2) were significantly increased in compound **1**- and **2**-treated cells. The presence of these oligomannose structures is highly indicative of cytosolic α-mannosidase inhibition since import to the lysosome from the cytosol is restricted to M_5N species [15]. MALDI mass spectrometry confirmed that the oligomannose structures containing 6–9 mannose residues had a single terminal *N*-acetylglucosamine residue (results not

Table 1 Structural assignment of 2-AA-labelled oligosaccharides separated by NP-HPLC

Peak number	Glucose unit	Proposed structure	Notes
1	3.9	$Man_3GlcNAc_1$	Core
2	4.2	$Man_3GlcNAc_2$	
3	4.9	$Man_4GlcNAc_1$	
4	5.1	$Man_4GlcNAc_2$	
5	5.75	$Man_5GlcNAc_1$	
6	5.85	$Man_5GlcNAc_1$	
7	6.0	$Man_5GlcNAc_1$	Ribo B structure
8	6.2	$Man_5GlcNAc_2$	
9	6.6	$Glc_1Man_5GlcNAc_1$	
10	6.9	$Man_6GlcNAc_1$	
11	7.1	$Man_6GlcNAc_1$	
12	7.3	$Man_6GlcNAc_2$	
13	7.6	$Man_7GlcNAc_{1\text{-}2}$	7b′ (-D1 & D3)
14	7.8	$Man_7GlcNAc_{1\text{-}2}$	
15	8.5	$Man_8GlcNAc_{1\text{-}2}$	8b′ (-D3)
16	8.8	$Man_8GlcNAc_{1\text{-}2}$	8a′ (-D2)
17	9.6	$Man_9GlcNAc_{1\text{-}2}$	
18	10.5	$Glc_1Man_9GlcNAc_1$	

Peak numbers refer to those in Figs. 2–4. Other than structures where the reducing terminus is either 1 or 2 GlcNAc residues ($GlcNAc_{1–2}$), identity was confirmed by enzyme digestion and/or MALDI mass spectrometry [15]. Peak 1 is a core-type structure, *i.e.*, Manα6(Manα3) Manß4GlcNAc and Peak 7 is the man5 isomer found in ribonuclease B (ribo B), *i.e.*, Manα6(Manα3)manα6(Manα3)Manß4GlcNAc

The nomenclature shown in the notes refers to the structure below

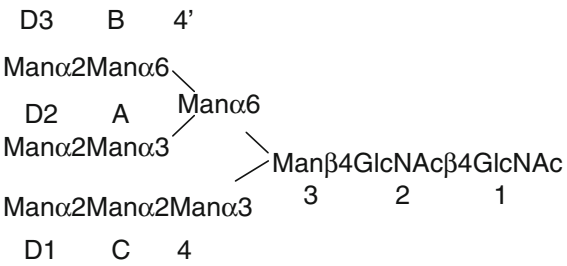

shown). The accumulation of larger oligomannosidic FOS in **1**- and **2**- treated cells was similar to mannosidase inhibition using DIM, DMJ and swainsonine (Fig. 3C, D, E). DIM was reported to be the most potent cytosolic α-mannosidase inhibitor known [17]. Results here have demonstrated that DIM is a much weaker inhibitor of cytosolic α-mannosidase than compounds **1** and **2**. Treatment of HL60 cells with DIM at 100 μM produced a ~1.5-fold increase in $M_{6–9}N_1$ species. In addition there were no significant changes in the $M_{4–5}N_1$ cytosolic species. These results demonstrated a very weak, partial inhibition of cytosolic α-mannosidase that was insufficient to affect major changes in all cytosolic intermediates. DMJ was an even weaker inhibitor of α-mannosidase in HL60 cells and the increase in FOS was negligible at 100 μM. At concentrations of 1 mM DMJ, a two-fold increase in total FOS (Fig. 3D) was observed. Swainsonine by contrast, prevented α-mannosidase hydrolysis in HL60 cells leading to M_5N_1 (Peak 7, Fig. 3) as a result of exclusive lysosomal-accumulation of hybrid structures following Golgi mannosidase II inhibition [18], and $M_{6–9}N_1$ species that could have been derived from either lysosomal or cytosolic inhibition or both. The results described later using MDBK cells suggest that lysosomal inhibition is the major source of these oligosaccharides leading to a six-fold increase. Kifunensine had little or no effect on FOS production in HL60 cells (Fig. 3B).

Compounds **3** and **4** can be seen as deoxy analogs of compounds **1** and **2** (Fig. 1). Both **3** and **4** generated lower amounts of $M_{6–9}N_1$ FOS species compared to **1** and **2** but produced a significant increase in M_5N_1 (Peak no. 6, Fig. 2D, E), M_4N_1 (Peak 3, Fig. 2D, E) and M_3N_1 species (Peak 1, Fig. 2D, E). These structures are predicted to accumulate in response to broad specificity α-mannosidase inhibition in the lysosome following the import of FOS

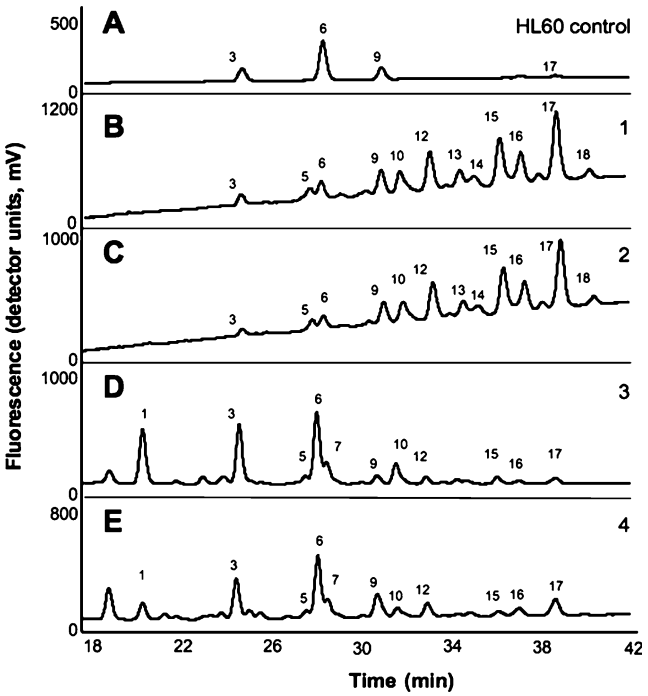

Fig. 2 Free Oligosaccharides (FOS) following azepane treatment of HL60 cells. Cells were treated for 24 h with **A** no inhibitor; **B** 100 μM **1**; **C** 100 μM **2**: **D** 100 μM **3**; **E** 100 μM **4**, free oligosaccharides purified, labelled with 2-AA and analysed by NP-HPLC. See Table 1 for assignment of structure to peak numbers

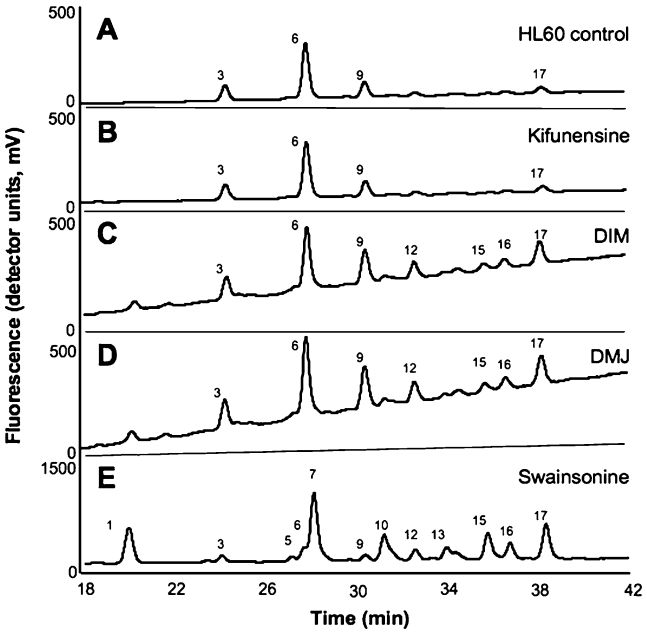

Fig. 3 Free Oligosaccharides (FOS) following mannosidase inhibitor treatment of HL60 cells. Cells were treated for 24 h with **A** no inhibitor; **B** 100 μM kifunensine; **C** 100 μM DIM: **D** 1 mM DMJ; **E** 100 μM swainsonine, free oligosaccharides purified, labelled with 2-AA and analysed by NP-HPLC. See Table 1 for assignment of structure to peak numbers

from the ERAD pathway (M_5N_1) and N-linked glycoproteins from the cell. These results were confirmed by *in vitro* enzyme analyses (see Table 2).

Effect of α-mannosidase inhibitors on FOS in MDBK cells

Compounds **1** and **2** at 100 μM for 24 h in MDBK cells resulted in a 14-fold increase in the core-type M_3N_2 oligosaccharide (Peak 2, Fig. 4A, B, C) indicating inhibition of α-mannosidase activity following glycoprotein influx to the lysosome [12]. Further increases in mannosylated *N*-acetylchitobiose structures, M_4N_2 and M_5N_2 (Peaks 4 and 8, Fig. 4) and a series of larger structures $M_{6-9}N_{1-2}$ (Peaks 12, 13, 14, 15, 16, 17, Fig. 4B, C) were observed. NP-HPLC does not resolve larger structures containing either a single *N*-acetylglucosamine or *N*-acetylchitobiose reducing terminus to allow unambiguous assignment, but the appearance of oligosaccharides with identical elution times in HL60 cells following treatment with **1** and **2** leads us to the conclusion that the larger mannosylated oligosaccharides were observed as a result of cytosolic mannosidase inhibition.

MDBK cells treated with **3** and **4** at 100 μM showed similarity in the free oligosaccharide profiles. By contrast to both lysosomal and cytosolic mannosidase inhibition displayed by **1** and **2**, only the lysosomal enzyme was inhibited, generating core-type M_3N_2 oligosaccharide (Peak 2, Fig. 4D, E). Both compounds increased by four-fold M_5N_1 oligosaccharide (Peak 6, Fig. 4) originating from the ERAD pathway suggesting that the breakdown of this oligosaccharide was also inhibited following transport into the lysosome, similar to observations in HL60 cells.

In MDBK cells compounds **1** and **2** at 100 μM had similar qualitative effects to DMJ at 1 mM (Fig. 4D, E and Fig. 5D) but the quantity of free oligosaccharide generated

Table 2 Inhibition of α-mannosidase activity

Inhibitor	Mannosidase activity (% of control)	
	pH 4.5	pH 6.5
Kifunensine	93.6±0.3	52.4±3.2
DIM	17.2±1.4	30.8±2.1
DMJ	99.6±0.4	60.4±4.2
Swainsonine	2.3±1.6	34.8±2.7
1	98.9±0.4	21.2±1.2
4	23.2±2.9	63.8±2.4

Rat liver homogenate was used as the enzyme source and assayed in 50 mM citric acid/sodium phosphate buffer containing 3 mM PNP-α-mannoside at pH 4.5 and pH 6.5 in the presence or absence of inhibitor (100 μM). *p*-Nitrophenol release was quantified at 400 nm and activity expressed as a percentage of a control, untreated sample

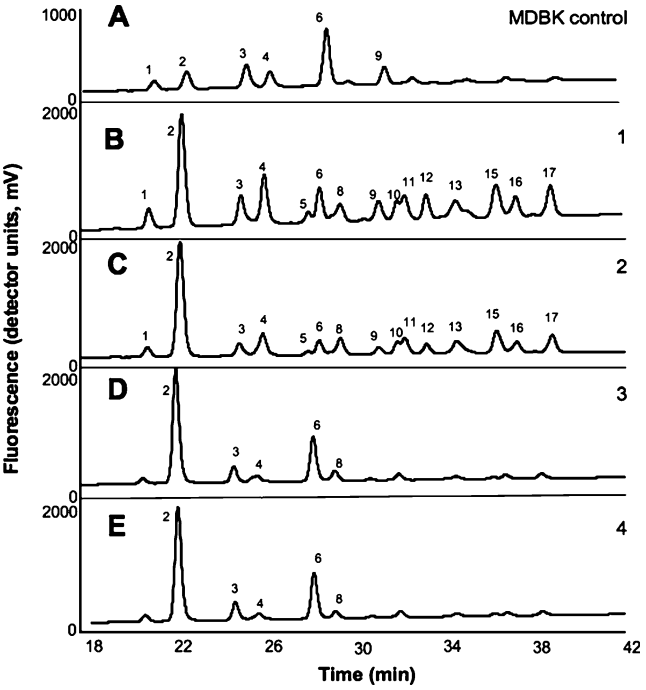

Fig. 4 Free Oligosaccharides (FOS) following azepane treatment of MDBK cells. Cells were treated for 24 h with **A** no inhibitor; **B** 100 μM **1**; **C** 100 μM **2**: **D** 100 μM **3**; **E** 100 μM **4**, free oligosaccharides purified, labelled with 2-AA and analysed by NP-HPLC. See Table 1 for assignment of structure to peak numbers

was four-fold greater, supporting the more potent inhibition of lysosomal α-mannosidase by the azepanes. DIM was more effective at inhibiting lysosomal mannosidase than the cytosolic enzyme in MDBK cells, as shown by the increase in core-type M_3N_2 oligosaccharide (Peak 2, Fig. 5C). The α(1,2), α(1,3) and α(1,6) activities of lysosomal mannosidase appear equally inhibited, characteristic of the deficiency in genetic α-mannosidosis of bovine and feline cells, and consistent with the known effects of DIM [19]. A similar increase in core-type oligosaccharides (7.8 fold) was obtained using swainsonine (Fig. 5E), the major species being M_5N_2 (Peak 8, Fig. 5E). As in HL60 cells, the latter species is stored lysosomally as a result of Golgi mannosidase II inhibition producing a greater incidence of N-linked hybrid structures, but with a *N*-acetylchitobiose reducing terminus.

Kifunensine treatment of MDBK cells at 1–100 μM produced a significant change in the FOS profile, more striking at 100 μM (Fig. 5B) where there was a 36-fold increase in M_8N_2 (8b′ isomer, D3 mannose missing, Fig. 5B Peak 15) oligosaccharide. Kifunensine is a very weak lysosomal mannosidase inhibitor [7], see Table 2, indicating that this M_8N_2 species was the product of ER α-mannosidase II hydrolysis, not ER mannosidase I which produces the 8a′ isomer (D2 mannose missing). This suggests that ER mannosidase I was strongly inhibited by

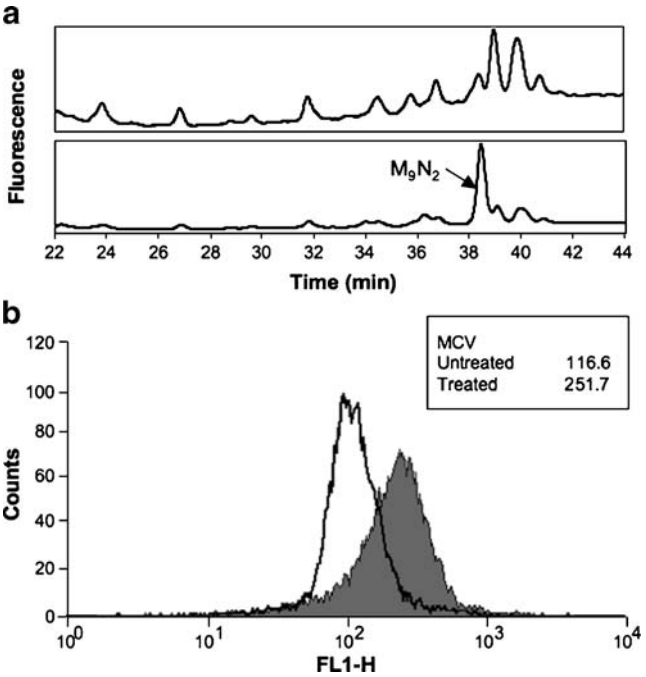

Fig. 6 Effects of kifunensine on cellular glycoprotein biosynthesis. HL60 cell glycoprotein oligosaccharides were released using PNGase, 2-AA labelled and analysed by NP-HPLC. **A** *top panel*, untreated cells; *lower panel*, cells treated for 24 h with 100 μM kifunensine. **B** Flow cytometry analysis of ConA reactive cells, untreated (*solid line*) and treated with 100 μM kifunensine for 24 h (*broken line*)

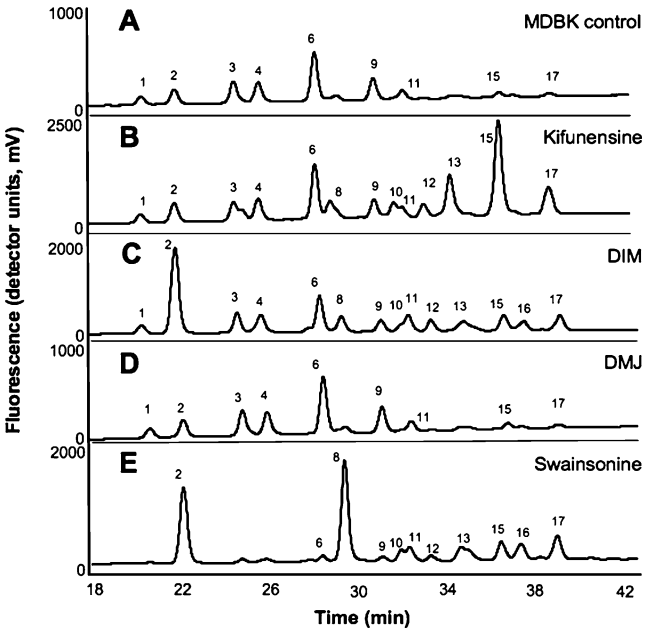

Fig. 5 Free Oligosaccharides (FOS) following mannosidase inhibitor treatment of MDBK cells. Cells were treated for 24 h with **A** no inhibitor; **B** 100 μM kifunensine; **C** 100 μM DIM: **D** 1 mM DMJ; **E** 100 μM swainsonine, free oligosaccharides purified, labelled with 2-AA and analysed by NP-HPLC. See Table 1 for assignment of structure to peak numbers

KIF and that these oligosaccharides could either accumulate in the ER or the cytosol, and not the lysosome. The presence of the *N*-acteylchitobiose core for the large mannosylated structures (determined following MALDI mass spectrometry analysis of isolated peaks, results not shown), supports the lack of exposure to cytosolic chitobiase activity that generates M_5N_1 as a result of ERAD (Fig. 5A Peak 6), which is therefore indicative of an ER-lumen localisation for the M_8N_2 isomer. Free mannosylated oligosaccharides could be generated by a decrease in ERAD following the disruption of mannosidase I activity by kifunensine [20] and reduction in the export of oligosaccharides to the cytosol, where inhibition of the cytosolic mannosidase is also poor (Table 2). These data also suggest that increases in M_8N_2 and other free oligosaccharides M_9N_2 (Fig. 5B Peak 17), M_7N_2 (7b′ isomer, D1 and D3 mannoses missing, Fig. 5B Peak 13) and $M_{5-6}N_2$ (Fig. 5B Peaks 8 and 12) are due to the lack of subsequent ER-processing of these structures. The further hydrolysis of M_9 and M_8 oligosaccharides occurs via ER-mannosidase I independent pathways, possibly involving M_9-α-mannosidase [20, 21].

The ER accumulation of these oligosaccharides points to greater non-proteasomal degradation of glycoproteins in MDBK cells since in HL60 cells the production of free

oligosaccharides was unaffected by kifunensine (Fig. 3). However, kifunensine was still an effective inhibitor of ER-mannosidase I processing of glycoproteins in HL60 cells. Analysis of treated cells by flow cytometry showed increased expression (two-fold after 24 h treatment) of mannosylated structures binding to ConA and the identification by NP-HPLC of a major peak corresponding to M_9N_2 oligosaccharide released from these cells by PNGase, confirmed ER-mannosidase inhibition by kifunensine (Fig. 6). Compound **1** by contrast, increased ConA binding marginally (1.2-fold) and the oligosaccharide profile was unchanged following treatment and was similar to control cells (Fig. 6, results not shown).

Structure-activity relationships

Structures of human ER mannosidase I in complex with kifunensine and DMJ [22] and *Drosophila* Golgi α-mannosidase II [23] have provided insight into the specificity of Class I and II α-mannosidases. DIM and SW modelled on the ER mannosidase I structure showed steric clashes of the pyranose ring with the side chain, which may partly explain why the larger 7-membered ring imino sugars poorly inhibit class I α-mannosidases in the biosynthetic pathway.

It is at present unclear why the azepanes, with glucose and idose-like stereochemistry's, have α-mannosidase inhibitory activity. As compounds **1-4** are all mannosidase inhibitors, the shared hydroxyl pattern at C-3, C-4 and C-5 is probably responsible for this inhibition, the size of the ring and its enhanced flexibility [24] possibly positioning these three hydroxyl groups rather ideally to mimic the mannopyranosidic substrate. Compared to known mannose-like imino sugars, the azepanes are more potent inhibitors of Class II α-mannosidases and this may be due to the geometry of the ring forming additional non-specific, weak interactions with the protein. The inhibition specificity is likely dependent on the nature and stereochemistry of the C6 group on the ring. Compounds **1** and **2** inhibit cytosolic α-mannosidase potently, suggesting that the hydroxymethyl group at C6 makes electrostatic interactions with specific side chains independent of stereochemistry. The specificity of **3** and **4** for lysosomal α-mannosidase on the other hand may reflect the presence of a hydrophobic moiety at or near the enzyme-binding site that preferentially interacts with a small non-polar methyl group. The chirality of this substituent however, seems to have some effect on the potency of α1,6 mannosidase inhibition.

Conclusion

The analysis of free oligosaccharides generated in response to inhibition of glycosidases is a powerful tool to compare the effects of compartmentalised inhibition in the cell [15]. We have shown here that this technique can be extended to mannosidase inhibition by evaluating the effects produced by a number of well-characterised imino sugars and novel azepanes. These data have provided an indication of the changes induced during the metabolism of N-linked glycoproteins in various subcellular compartments. Further experiments to unambiguously determine FOS localisation will be required to confirm the present studies and cell fractionation studies are in progress to address this issue. Inhibitors with hydroxymethyl groups at C6, compounds **1** and **2** (Fig. 1) show remarkable selectivity for the inhibition of cytosolic α-mannosidase and free oligosaccharides produced from the ERAD pathway can be clearly distinguished from those of lysosomal, ER and Golgi origin by comparing the analysis in normal and lysosomal enzyme deficient cells. Cellular studies such as these have considerable value in the design of imino sugars as potential therapeutic agents where enzyme selectivity, cellular uptake and organelle penetration are critical issues that can be rapidly and robustly addressed.

Acknowledgements The authors thank Prof. Raymond Dwek and the Glycobiology Institute for support.

References

1. Daniel, P.F., Winchester, B., Warren, C.D.: Mammalian alpha-mannosidases–multiple forms but a common purpose. Glycobiology **4**, 551–566 (1994). doi:10.1093/glycob/4.5.551
2. Winchester, B., Fleet, G.W.: Amino-sugar glycosidase inhibitors: versatile tools for glycobiologists. Glycobiology **2**, 199–210 (1992). doi:10.1093/glycob/2.3.199
3. Asano, N., Kato, A., Watson, A.A.: Therapeutic applications of sugar-mimicking glycosidase inhibitors. Mini Rev. Med. Chem. **1**, 145–154 (2001). doi:10.2174/1389557013407052
4. Goss, P.E., Reid, C.L., Bailey, D., Dennis, J.W.: Phase IB clinical trial of the oligosaccharide processing inhibitor swainsonine in patients with advanced malignancies. Clin. Cancer Res. **3**, 1077–1086 (1997)
5. Li, H., Liu, T., Zhang, Y., Favre, S., Bello, C., Vogel, P., Butters, T.D., Oikonomakos, N.G., Marrot, J., Blériot, Y.: New synthetic seven-membered 1-azasugars displaying potent inhibition towards glycosidases and glucosylceramide transferase. ChemBioChem **9**, 253–260 (2008). doi:10.1002/cbic.200700496
6. Herscovics, A.: Processing glycosidases of Saccharomyces cerevisiae. Biochim. Biophys. Acta **1426**, 275–285 (1999)
7. Spiro, R.G.: Role of N-linked polymannose oligosaccharides in targeting glycoproteins for endoplasmic reticulum-associated degradation. Cell. Mol. Life Sci. **61**, 1025–1041 (2004). doi:10.1007/s00018-004-4037-8
8. Wiertz, E.J., Tortorella, D., Bogyo, M., Yu, J., Mothes, W., Jones, T.R., Rapoport, T.A., Ploegh, H.L.: Sec61-mediated transfer of a membrane protein from the endoplasmic reticulum to the proteasome for destruction. Nature **384**, 432–438 (1996). doi:10.1038/384432a0
9. Oda, Y., Hosokawa, N., Wada, I., Nagata, K.: EDEM as an acceptor of terminally misfolded glycoproteins released from

calnexin. Science **299**, 1394–1397 (2003). doi:10.1126/science.1079181
10. Suzuki, T.: Cytoplasmic peptide:N-glycanase and catabolic pathway for free N-glycans in the cytosol. Semin. Cell Dev. Biol. **18**, 762–769 (2007). doi:10.1016/j.semcdb.2007.09.010
11. Suzuki, T., Hara, I., Nakano, M., Shigeta, M., Nakagawa, T., Kondo, A., Funakoshi, Y., Taniguchi, N.: Man2C1, an alpha-mannosidase, is involved in the trimming of free oligosaccharides in the cytosol. Biochem. J. **400**, 33–41 (2006). doi:10.1042/BJ20060945
12. Winchester, B.: Lysosomal metabolism of glycoproteins. Glycobiology **15**, 1R–15R (2005). doi:10.1093/glycob/cwi041
13. Park, C., Meng, L., Stanton, L.H., Collins, R.E., Mast, S.W., Yi, X., Strachan, H., Moremen, K.W.: Characterization of a human core-specific lysosomal {alpha}1,6-mannosidase involved in N-glycan catabolism. J. Biol. Chem. **280**, 37204–37216 (2005). doi:10.1074/jbc.M508930200
14. Abraham, D., Blakemore, W.F., Jolly, R.D., Sidebotham, R., Winchester, B.: The catabolism of mammalian glycoproteins. Comparison of the storage products in bovine, feline and human mannosidosis. Biochem. J. **215**, 573–579 (1983)
15. Alonzi, D.S., Neville, D.C., Lachmann, R.H., Dwek, R.A., Butters, T.D.: Glucosylated free oligosaccharides are biomarkers of endoplasmic- reticulum alpha-glucosidase inhibition. Biochem. J. **409**, 571–580 (2008). doi:10.1042/BJ20070748
16. Neville, D.C., Coquard, V., Priestman, D.A., te Vruchte, D.J., Sillence, D.J., Dwek, R.A., Platt, F.M., Butters, T.D.: Analysis of fluorescently labeled glycosphingolipid-derived oligosaccharides following ceramide glycanase digestion and anthranilic acid labeling. Anal. Biochem. **331**, 275–282 (2004). doi:10.1016/j.ab.2004.03.051
17. Weng, S., Spiro, R.G.: Endoplasmic reticulum kifunensine-resistant alpha-mannosidase is enzymatically and immunologically related to the cytosolic alpha-mannosidase. Arch. Biochem. Biophys. **325**, 113–123 (1996). doi:10.1006/abbi.1996.0014
18. Moremen, K.W.: Golgi alpha-mannosidase II deficiency in vertebrate systems: implications for asparagine-linked oligosaccharide processing in mammals. Biochim. Biophys. Acta **1573**, 225–235 (2002)
19. Daniel, P.F., Newburg, D.S., O'Neil, N.E., Smith, P.W., Fleet, G. W.: Effects of the alpha-mannosidase inhibitors, 1,4-dideoxy-1,4-imino-D-mannitol and swainsonine, on glycoprotein catabolism in cultured macrophages. Glycoconj. J. **6**, 229–240 (1989). doi:10.1007/BF01050651
20. Avezov, E., Frenkel, Z., Ehrlich, M., Herscovics, A., Lederkremer, G.Z.: Endoplasmic reticulum (ER) mannosidase I is compartmentalized and required for N-glycan trimming to Man5-6GlcNAc2 in glycoprotein ER-associated degradation. Mol. Biol. Cell **19**, 216–225 (2008). doi:10.1091/mbc.E07-05-0505
21. Bieberich, E., Bause, E.: Man9-mannosidase from human kidney is expressed in COS cells as a Golgi-resident type II transmembrane N-glycoprotein. Eur. J. Biochem. **233**, 644–649 (1995). doi:10.1111/j.1432-1033.1995.644_2.x
22. Vallee, F., Karaveg, K., Herscovics, A., Moremen, K.W., Howell, P.L.: Structural basis for catalysis and inhibition of N-glycan processing class I alpha 1,2-mannosidases. J. Biol. Chem. **275**, 41287–41298 (2000). doi:10.1074/jbc.M006927200
23. van den Elsen, J.M., Kuntz, D.A., Rose, D.R.: Structure of Golgi alpha-mannosidase II: a target for inhibition of growth and metastasis of cancer cells. EMBO J **20**, 3008–3017 (2001). doi:10.1093/emboj/20.12.3008
24. Martinez-Mayorga, K., Medina-Franco, J.L., Mari, S., Canada, F. J., Rodriguez-Garcia, E., Vogel, P., Li, H., Blériot, Y., Sinaÿ, P., Jimenez-Barbero, J.: The conformational behavior of novel glycosidase inhibitors with substituted azepan structures : a NMR and modeling study. Eur. J. Org. Chem. **20**, 4119–4129 (2004). doi:10.1002/ejoc.200400320